Frederik Kurzrock[1], Andrea Hochebner[1], Quentin Millerioux[1], Nicolas Schmutz[1], Maria Reinhardt[2], Walter Acevedo[2], Roland Potthast[2]

[1]Reuniwatt SAS, Sainte Clotilde, France
[2]Deutscher Wetterdienst, Offenbach, Germany

Contact: icamcloudops@reuniwatt.com

The project ICamCloudOps is funded by:

mFUND – Das Startkapital für die Mobilität 4.0

Bundesministerium für Verkehr und digitale Infrastruktur

# Nudging with sky imager observed clouds can improve hour-scale WRF forecasts.

## Observed cloud cover

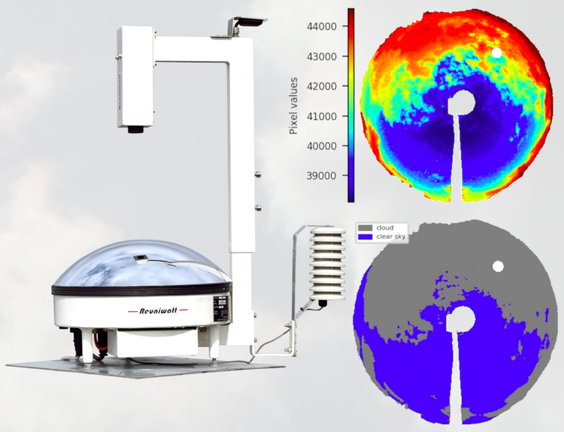



Fig. 1: Reuniwatt's all-sky imager Sky InSight™ (left) operates in thermal infrared (top right) and can provide a cloud mask (lower right) at day and night time.

## Humidity profile

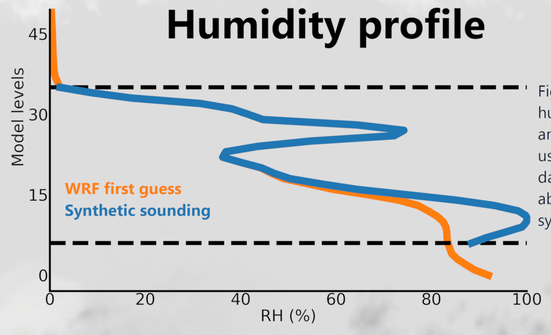



Fig. 2: WRF profile of relative humidity before nudging (orange) and synthetic radio sounding used for nudging (blue). The dashed lines show the limits above and below which the synthetic sounding is undefined.

## FDDA Nudging

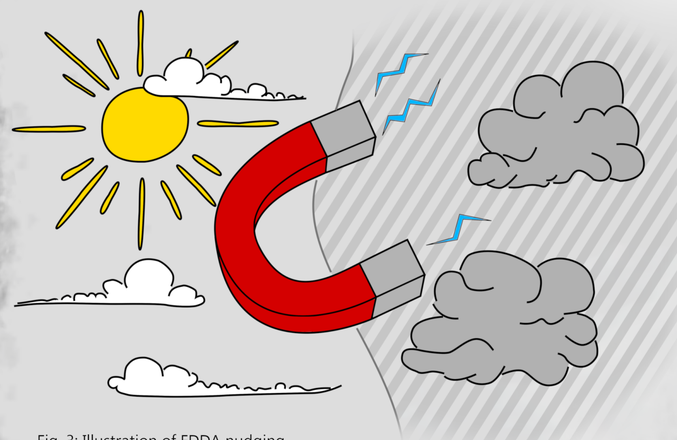


Fig. 3: Illustration of FDDA nudging.

## Cloud cover forecast

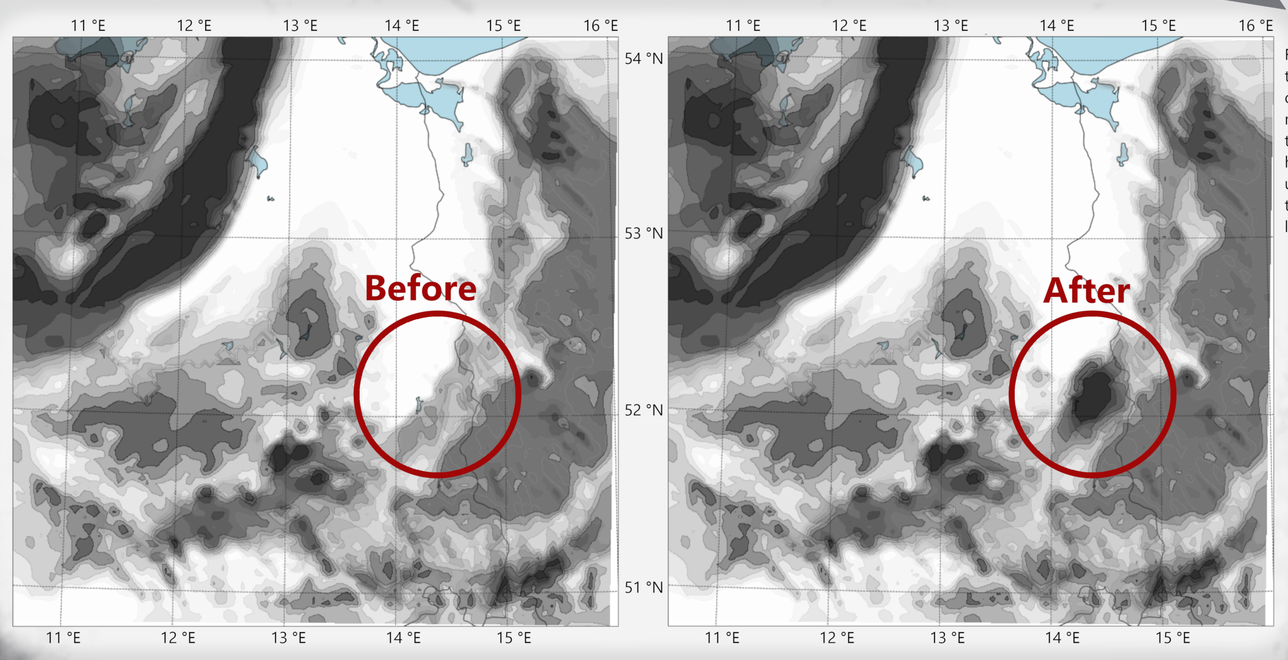



Fig. 4: Example of the impact of the FDDA nudging approach on cloud cover (before and after nudging). For illustrative reasons the nudging configuration that has been used for this figure uses higher nudging weights than the one used in the long-term experiments.

## 1) Motivation

Numerical weather prediction (NWP) models such as the Weather Research and Forecasting (WRF) model allow to forecast cloud processes at high spatio-temporal resolutions of a few kilometres and minutes. Nevertheless, WRF is known to underestimate the presence of clouds, which has negative impacts on solar irradiance forecasts for example. Therefore, drawing the forecasts closer to observations of clouds can be an efficient means for improving hour-scale cloudiness forecasts.

Determining precise initial conditions from both observations and model output in terms of clouds is a challenge. While sophisticated variational and ensemble-based data assimilation methods are being continuously improved, four-dimensional data assimilation (FDDA) Nudging is an often neglected, simple, and cost-effective data assimilation approach (Fig. 3).

This study explores the use of FDDA nudging to take into account cloud cover observations from an infrared all-sky imager in forecasts of the Weather Research and Forecasting (WRF) model. Reuniwatt's thermal infrared all-sky imager Sky InSight™ (Fig. 1) retrieves cloud properties such as cloud fraction (Baidar et al. 2020) with constant accuracy at day and night.

## 2) WRF configuration

WRF version 4.4 (Skamarock et al. 2019) has been used for both reference and nudging experiments with a one-way nesting two domain setup (9 km and 3 km grid spacing) over Central Europe (Fig. 5), driven by Global Forecasting System (GFS) forecasts. One forecast per day has been performed for April and May 2022, initialised with the 00Z GFS run with a maximum lead time of 24 h. A total of 15 days with actual nudging are considered.
Features of the configuration:

Domain size: approx. 125 x 125 grid boxes for both domains
Microphysics: Thompson
Long-wave and short-wave radiation: RRTMG
PBL physics: MYNN
Cumulus: Kain-Fritsch

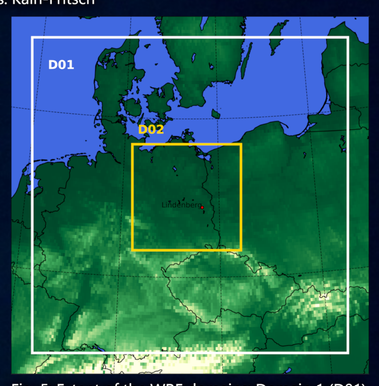



Fig. 5: Extent of the WRF domains: Domain 1 (D01) with a grid spacing of 9 km and one-way nested domain 2 (D02) with a grid spacing of 3 km.

## 3) Experiment setup

The WRF built-in four-dimensional data assimilation (FDDA) observation nudging funtionality has been used to nudge the model towards synthetic radio soundings of relative humidity (Fig. 2 and 3) at Lindenberg, Germany (in the red circle in Fig. 4). Depending on the difference between the WRF first guess and the synthetic sounding, clouds are either added or removed. Please excuse us for not providing details about the creation method of the synthetic profiles since it is subject of an ongoing patent filing. The WRF FDDA observation nudging creates an innovation (difference between model and observation) which is added to model tendencies to gradually nudge the model towards the observation following the equation (Dudhia 2018):

$$\frac{\partial q\mu}{\partial t}(x,y,z,t) = \underbrace{F_q(x,y,z,t)}_{\text{Tendency in grid box before nudging}} + \mu \underbrace{G_q}_{\text{General weight term (nudging strength)}} \frac{\overbrace{\sum_{i=1}^{N} W_q^2(i,x,y,z,t)}^{\text{Spatiotemporal weighting function}} \overbrace{[q_0(i) - q_m(x_i,y_i,z_i,t)]}^{\text{Innovation}}}{\sum_{i=1}^{N} W_q(i,x,y,z,t)}$$

A general weight term of 6.40E-03, a temporal weight of 30 min, and a spatial weight (influence radius) of 15 km have been applied.

## 4) Spatial verification method

The spatial verification of the WRF cloud cover forecasts is performed using Reuniwatt's custom Meteosat Second Generation (MSG) Satellite Application Facility NoWCasting (SAFNWC) cloud mask (Derrien and Le Gléau 2005). A WRF cloud mask is generated using a column based cloud cover threshold of 0.2. Both WRF and satellite
data are reprojected to the same rectilinear grid (EPSG4326).

The spatial verification is based on contingency table values:

| | | Satellite | |
|---|---|---|---|
| | Scenario | Clear | Cloudy |
| WRF | Clear | a | b |
| | Cloudy | c | d |

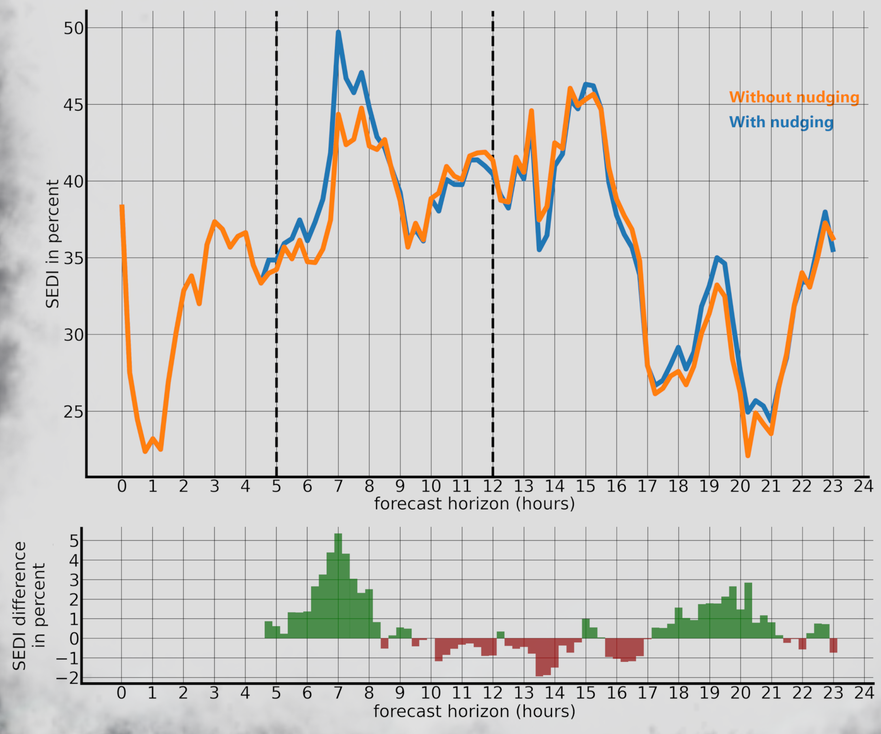
Table 1: Cloud mask contingency table for WRF and satellite clouds.

The Symmetric Extremal Dependency Index (SEDI) is used as spatial verification metric (Gregow et al. 2020). It is defined as:

$$SEDI = \frac{\log F - \log H - \log(1-F) + \log(1-H)}{\log F + \log H + \log(1-F) + \log(1-H)} \times 100\%$$

with H and F being:

$$H = \frac{a}{a+c} \qquad F = \frac{b}{b+d}$$




## Long-term spatial verification

Fig. 6: The top plot shows a comparison of SEDI for the WRF experiments in domain 2 without nudging (blue) and with nudging (orange) for the study period of 15 individual days in April and May 2022 per forecast horizon. The vertical dashed lines indicate the times between which FDDA nudging has been performed.
The bottom plot shows the difference between the two lines in the upper plot, meaning positive impact (green) and negative impact (red) per forecast horizon.

## 5) Results

The impact of the nudging on cloud cover forecasts is illustrated with ground-based solar irradiance observations for an example day (5.1) and a long-term satellite-based spatial verification (5.2):

### 5.1) Solar irradiance case study

On 30 April 2022 the initial WRF forecast contained almost no clouds above Lindenberg until 12Z, resulting in almost a clear-sky global horizontal irradiance (GHI) curve (green line in Fig. 7). Ground-based sky images reveal a closed layer of high clouds in the morning (Fig. 8). Nudging was performed several times between 05Z and 12Z (yellow lines in Fig. 7) resulting in augmented relative humidity in the upper troposphere and consequently less GHI (blue line in Fig. 7), bringing the forecast closer to the observations.

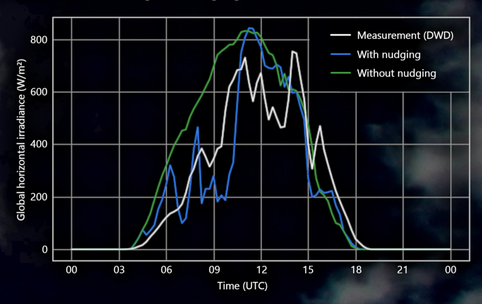



Fig. 7: Global horizontal irradiance at Lindenberg (Germany) on 30 April 2022 as measured (white), and forecasted by WRF in a first guess forecast (green) and after nudging (blue). The yellow lines indicate the times of nudging.



Fig. 8: DWD webcam image taken on 30 April 2022 at 08:30 UTC in Falkenberg (Germany) viewing in the direction of the Sky InSight (Fig. 2) showing high stratus clouds.

### 5.2) Spatial verification

For individual days, the impact of the nudging depends very much on the synoptic conditions and the wind speed which is causing clouds to either remain at the same location or move. This also affects the duration of the nudging impact after the nudging period. As explained in chapter 3, the nudging either adds or removes clouds. Both cases appear about as often within the study period and lead to an overall improvement of the WRF forecasts in terms of SEDI (Fig. 6). Nevertheless, a slight degradation of the forecasts is visible immediately after the nudging period, followed by another improvement.

## 6) Conclusion and Outlook

The experiments show promising results and an overall functioning setup and proof of concept. The assimilation of synthetic humidity profiles with FDDA nudging at just one single site has a significant impact on the cloud cover forecasts for the entire WRF domain. As the SEDI lines in Fig. 6 are still not very smooth, the study period should be extended to more days to obtain statistically more robust results. Moreover, it would be desirable to add more sites to the study.

### References

Baidar et al. (2020), Doppler wind lidar observations of shallow cumulus clouds, 100th AMS Annual Meeting, Boston, USA.
Derrien, M. and Le Gléau, H. (2005), MSG/SEVIRI cloud mask and type from SAFNWC, Int J Remote Sens 26, 4707–4732. https://doi.org/10.1080/01431160500166128
Dudhia, J. (2018), WRF Four-Dimensional Data Assimilation (FDDA), https://documen.site/download/wrffddadudhia_pdf
Gregow, E. et al. (2020), The use of satellite and surface observations for initializing clouds in the HARMONIE NWP model.
Skamarock et al. (2019), A Description of the Advanced Research WRF Version 4. NCAR Tech. Note NCAR/TN-556+STR, 145 pp. doi:10.5065/1dfh-6p97